

Numerical Approach to Space Charge Effects Simulation in Multi-Beam Irradiation for Heavy Ion Fusion

A.I. Ogoyski, P.H. Popov

Technical University of Varna, Varna 9010, Bulgaria

Received 19 May 2009

Abstract. Space charge effects in multi-beam irradiation play an important role for increasing the energy deposition entropy in inertial confinement fusion. The analytical approach is too complicated and leads to heavy and slow-working numerical procedures even in multiple-processor's performance. The proposed numerical algorithm is a simple and efficient iterative space charge effects evaluation, created to improve the OK2 code calculation accuracy.

PACS number: 52.58.Hm, 52.40.Mj, 28.52.Cx, 41.75.Ak, 41.85.Ja, 29.27.Eg

1 Introduction

Heavy ion beam (HIB) is one of the promising energy-driver candidates in inertial confinement fusion [1-13]. In heavy ion fusion (HIF) one of the key issues is HIB final transport in a gas-filled reactor chamber. The HIBs should be transported through the reactor gas in 2–6 m and focused on a fuel pellet of a radius of few mm. Direct-driven as well as indirect-driven fuel pellets require several MJ of HIB driver energy in HIF. Each HIB carries $\sim 1\text{--}5$ kA and HIB particle energy should be $\sim 4\text{--}10$ GeV depending on the HIB ion types. In case of Pb^+ HIB radius at the chamber beam port entrance can be 2–4 cm and its number density $n_{b0} \sim 10^{12} \text{ cm}^{-3}$. Propagating in the chamber HIB radius decreases to $R_b \sim 2\text{--}6$ mm and its number density increases to $n_{bf} \sim 100\text{--}200 \times n_{b0} = 1\text{--}2 \times 10^{14} \text{ cm}^{-3}$ at the fuel pellet position.

In the HIB final transport several transport schemes have been proposed: pre-formed channel transport [3-5], neutralized ballistic transport using a pre-formed plasmas [3,6,7], or using a tube liner [8-11], ballistic transport in near vacuum [3] and many other.

Nearly all of the above schemes describe one or two-beam irradiation on the fuel pellet and propose solutions to suppress the HIB divergence by the ambipolar

field at time of the beam propagation in the reactor chamber. The HIBs are ionized to $Z_b \sim 1-6$ depending on the transport conditions.

The most important results from these studies are included in OK2 code and described by the beam emittance [1,2]. However in case of multi-beam irradiation [12,13] HIBs start to overlap around the pellet and a dynamic non-uniform electric field is created from this effect. That electric field increases the deposition entropy at the time of irradiation and disturbs the ion ballistic trajectories. Analytic calculations of each ion trajectory are principally possible but will make the code too heavy and slow-working even if multiple processors are used. The purpose of the present study is to create a simple and appropriate numerical algorithm describing the space charge effects in multi-beam irradiation for HIF, and to improve the calculation accuracy of OK2 code.

2 Numerical Algorithm

The described numerical algorithm is a simple and efficient iterative space charge effects evaluation in HIF. Each beam is longitudinal subdivided into n_{bch} bunches [1,2] and the pellet surface consists of $n_\theta \times n_\phi$ number of meshes. The indexes $j = 1, 2, \dots, n_\theta$ and $k = 1, 2, \dots, n_\phi$ indicate the pellet meshes in θ and ϕ directions in spherical coordinates. First bunches (first one from each beam) just before to impinge on the pellet surface, overlap in a layer around the pellet and create a non-uniform electric field (see Figure 1). Even in totally neutralized ballistic transport schemes [3,6,7], near to the fuel pellet at the chamber center the HIB number density increases and we can expect additional ionization (especially in the overlapping area). We assume that the ions from the first bunches propagate on straight trajectories through the chamber. From that assumption the ion number density distribution on the pellet surface (due to the

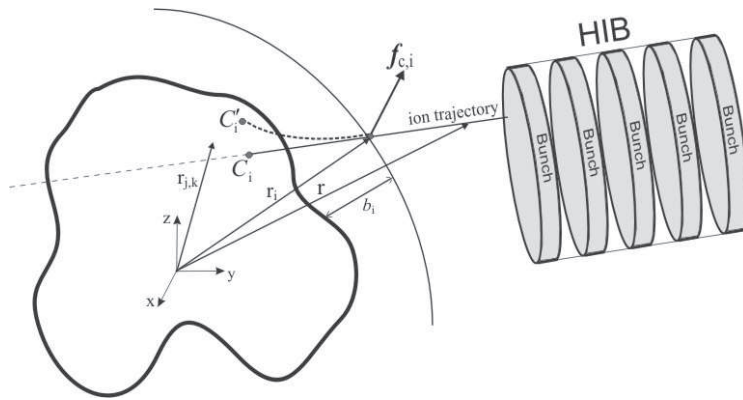


Figure 1. Space charge effects evaluation scheme.

ions from the first bunches) is evaluated. An ion from the second bunch obtains a potential energy $E_{p,2}$.

$$E_{p,2} = \frac{e^2 Z_{b,2} Z_{b,1}}{4\pi\epsilon\epsilon_0} \sum_j \sum_k \frac{N_1(j,k)}{|\vec{r} - \vec{r}_{j,k}|}, \quad (1)$$

where e is the electron charge magnitude, $\epsilon\epsilon_0$ is the reactor chamber gas permittivity, $Z_{b,1}$ and $Z_{b,2}$ are the electric charges of the ions from the first and second bunches and $N_1(j,k)$ is the number of ions from the first bunches in the surface mesh with index j,k . In a distance $\vec{r} = \vec{r}_2$ the potential energy $E_{p,2}$ takes value of $E_{k,2}$ (particle kinetic energy). We define the critical distance b_2 , then the ion trajectory closer to the pellet is affected from the electric field created around the pellet surface

$$b_2 = |\vec{r}_2| - \frac{\sum_j \sum_k |\vec{r}_{j,k}|}{n_\theta n_\phi}. \quad (2)$$

The value of b_2 can be interpreted as the effective thickness of the overlapping layer created around the pellet, due to the ions from the first bunches. The Coulomb force $\vec{f}_{c,2}$ acting on the ion from the second bunch in a distance b_2 is

$$\vec{f}_{c,2} = \frac{e^2 Z_{b,2} Z_{b,1}}{4\pi\epsilon\epsilon_0} \sum_j \sum_k \frac{N_1(j,k) (\vec{r}_2 - \vec{r}_{j,k})}{|\vec{r}_2 - \vec{r}_{j,k}|^3}. \quad (3)$$

The projection of $\vec{f}_{c,2}$ on the pellet surface determines the direction of the ion deflection from the intersection point C_2 (impinging point to the non-disturbed ion). Following that direction we find the point C'_2 where the potential energy of the ion will be minimal and assume that the ion impinges on that point. The boundary condition is the length of $C_2 C'_2$ not to exceed the effective thickness b_2 . Because of the short deposition time – 10 ns, we ignore the surface transport processes during that initial time. After the second bunch deposition upon, the electric field around the pellet changes and the ions from the next bunch are influenced from the new electric field that is created. For i -th bunch the ion deflections are determined by solving the system of equations (4):

$$\left\{ \begin{array}{l} E_{p,i} = \frac{e^2 Z_{b,i}}{4\pi\epsilon\epsilon_0} \sum_m = 1^{i-1} \left(Z_{b,m} \sum_j \sum_k \frac{N_m(j,k)}{|\vec{r}_i - \vec{r}_{j,k}|} \right) = E_{k,i} \\ b_i = |\vec{r}_i| - \frac{\sum_j \sum_k |\vec{r}_{j,k}|}{n_\theta n_\phi} \\ \vec{f}_{c,i} = \frac{e^2 Z_{b,i}}{4\pi\epsilon\epsilon_0} \sum_{m=1}^{i-1} \left(Z_{b,m} \sum_j \sum_k \frac{N_m(j,k) (\vec{r}_i - \vec{r}_{j,k})}{|\vec{r}_i - \vec{r}_{j,k}|^3} \right) \\ C_i C'_i \leq b_i \end{array} \right. \quad (4)$$

($i = 2, 3, 4, \dots, n_{\text{bch}}; \quad m = 1, 2, 3 \dots, n_{\text{bch}} - 1$)

3 Simulation Results

The space charge effects evaluation was included in OK2 code and tested on a simple simulation scenario. A spherical Al pellet was irradiated by three Pb^{+3} beams, with a difference of its impinging directions of 30 degrees from each one to another (see Figure 2a). Each beam has the following parameters: the beam radius at the chamber entrance is 35 mm and decreases to 2 mm at the pellet position, the beam particle density is in the Kapchinskii–Vladimirskii (KV) distribution and all ions have the same energy of 8 GeV (a cold beam), the maximal beam current is 5 kA, the pulse width is 10 ns with the rise and fall times of 2 ns [13]. In order to demonstrate only the space charge effects evaluation, the beam emittance (*i.e.* HIB transverse divergence by the ambipolar field) is set to be zero mm-mrad. The beam and pellet temperature effects are also excluded. Figure 2b shows the rise of the critical distance b_i for an ion from the center of HIB. As should be expected the tail ions from the HIB are disturbed much more than the front ions. The ion number density distributions at the pellet surface without space charge effects evaluation (see Figure 3a) and with space charge effects evaluation (see Figure 3b) are compared. The Coulomb spread is very well seen especially in the overlap area. The deposition picture becomes more realistic and the accuracy of OK2 calculations increases.

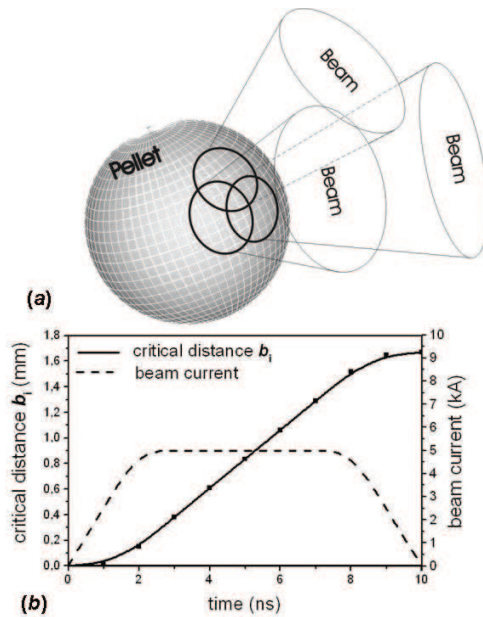


Figure 2. Three-beam irradiation on a spherical pellet: (a) irradiation scheme; (b) critical distance b_i and beam current at the time of deposition.

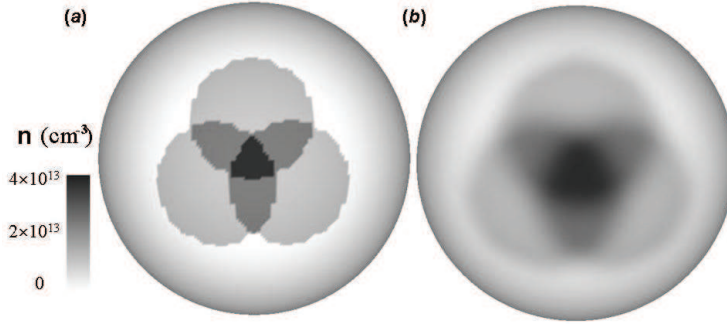


Figure 3. Ion number density distribution at the pellet surface: (a) without space charge effects evaluation; (b) with space charge effects evaluation.

To test the algorithm in a typical HIF simulation, the Al spherical pellet was irradiated by 32-beam central-symmetric system (based on dodecahedron [15-17]). The HIB parameters are the same as in the previous test. The energy deposition layer has external radius $R_0 = 4$ mm and thickness of 1 mm. It was subdivided into a mesh structure in the r , θ and φ directions with the following mesh numbers: $n_r = 100$, $n_\theta = 180$, $n_\phi = 360$. Each spherical shell layer has a thickness dr of 0.01 mm. For the energy deposition non-uniformity evaluation [2] we define the total relative root-mean-square (RMS) deviation σ_{RMS} and the total relative peak-to-valley (PTV) deviation σ_{PTV} as follows:

$$\sigma_{\text{RMS}} = \sum_i^{n_r} w_i \sigma_{\text{RMS}i}, \quad \sigma_{\text{RMS}i} = \frac{1}{\langle E \rangle_i} \sqrt{\frac{\sum_j^{n_\theta} \sum_k^{n_\phi} (\langle E \rangle_i - E_{ijk})^2}{n_\theta n_\phi}}, \quad w_i = \frac{E_i}{E}, \quad (5)$$

$$\sigma_{\text{PTV}} = \sum_i^{n_r} w_i \sigma_{\text{PTV}i}, \quad \sigma_{\text{PTV}i} = \frac{E_i^{\text{max}} - E_i^{\text{min}}}{2\langle E \rangle_i}, \quad (6)$$

where $\sigma_{\text{RMS}i}$ is the relative RMS deviation on the i -th spherical shell layer of the fuel pellet, E_i is the energy deposited on that shell and E is the total energy deposition, $\sigma_{\text{PTV}i}$ is the relative PTV deviation on the i -th shell layer, E_i^{max} and E_i^{min} are the maximal and minimal energy deposited on that shell. Figure 4 shows the non-uniformity evaluation and the energy deposition profile in pellet radial direction (radial cut of pellet deposition layer).

4 Discussions and Conclusions

The magnitude of the Coulomb spread is estimated quantitatively by the fall to σ_{PTV} four times. That effect decreases the non-uniformity of the energy deposition σ_{RMS} twice. All other effects (excluded from that simulation) which in-

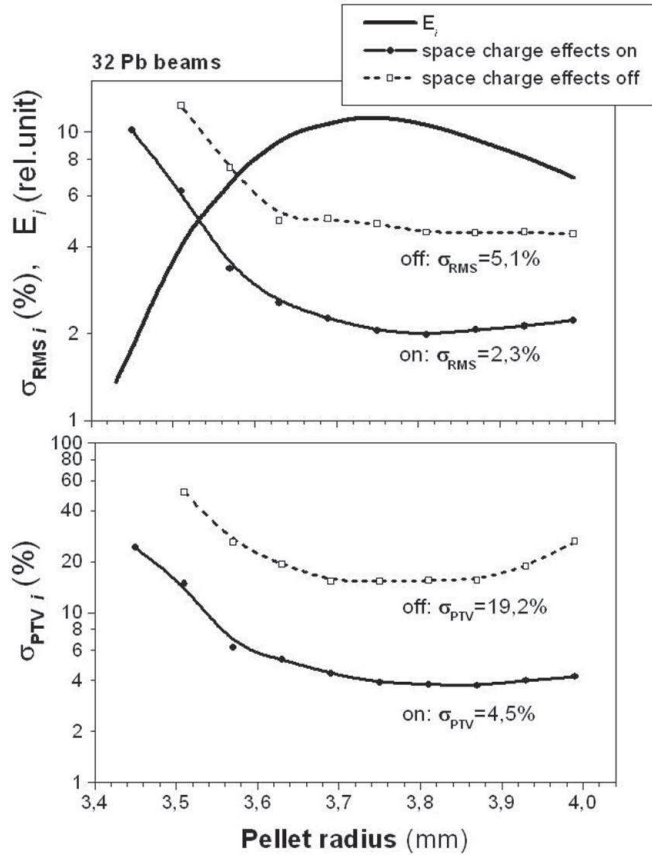


Figure 4. σ_{RMS_i} , σ_{PTV_i} and the energy deposition profile E_i versus the pellet radius.

crease the beam emittance and raise the pellet temperature during the deposition time have the same tendency to decrease the energy deposition non-uniformity. All of them diminish σ_{RMS} , but not so drastically σ_{PTV} . Therefore, in case of multi-beam irradiation simulations, the artificial non-uniformity might be generated by the code if the space charge effects (due to the beam overlapping) are ignored.

The presented numerical algorithm is based on energy conservation law and entropy increasing principle. It is simple, efficient and gives physical results with negligible slow up in code performance. The calculation accuracy of OK2 code is improved. As a result the energy deposition picture becomes more realistic.

References

- [1] A.I. Ogoyski, S. Kawata, T. Someya (2004) *CPC* **161** 143-150.
- [2] A.I. Ogoyski, S. Kawata, T. Someya (2004) *CPC* **157** 160-172.
- [3] D.A. Callahan (1995) *Appl. Phys. Lett.* **67** L3254.
- [4] D.A. Callahan (1996) *Fusion Eng. Des.* **441** 32.
- [5] R.R. Peterson, C.L. Olson (1997) *AIP Conference Proceedings* **259** 406.
- [6] W.M. Sharp, D.P. Grote, D.A. Callahan, et al. (2003) *Phys. Plasmas* **10** 2457.
- [7] P.K. Roy, S.S. Yu, E. Henestrosa, et al. (2004) *Phys. Plasmas* **11** 2890.
- [8] J. Sasaki, T. Nakamura, T. Uchida, T. Someya, K. Shimizu, K. Shitamura, T. Teramoto, A.B. Blagoev, S. Kawata (2001) *Jap. J. Appl. Phys.* **40** 968-971.
- [9] T. Someya, S. Kawata, T. Nakamura, A.I. Ogoyski, K. Shimizu, J. Sasaki (2003) *Fusion Sci. Technol.* **43** 282-289.
- [10] C. Deutsch, S. Kawata, T. Nakamura (2001) *J. Plasma Fusion Rev.* **77** 33.
- [11] W.B. Herrmannsfeidt (2001) *Nucl. Instrum. Methods Phys. Res., Sect. A* **464** 305.
- [12] A.I. Ogoyski, T. Someya, T. Sasaki, S. Kawata (2003) *Phys. Let. A* **315** 372-377.
- [13] A.I. Ogoyski, S. Kawata, T. Someya, A.B. Blagoev, P. Popov (2004) *J. Phys. D* **37** 2392-2394.
- [14] S. Kawata, T. Someya, T. Nakamura, S. Miyazaki, K. Shimizu, A.I. Ogoyski (2003) *Laser and Particle Beams* **21** 27-32.
- [15] M. Murakami (1995) *Appl. Phys. Lett.* **66** 1587.
- [16] S. Skupsky, J. Lee (1983) *Appl. Phys.* **54** 3662.
- [17] M. Murakami, J. Meyer-ter-Vehn (1991) *Nuclear Fusion* **31** 7.